

# Surface Features of Recombinant Spider Silk Protein eADF4( $\kappa$ 16)-Made Materials are Well-Suited for Cardiac Tissue Engineering

Jana Petzold, Tamara B. Aigner, Filip Touska, Katharina Zimmermann, Thomas Scheibel, and Felix B. Engel\*

Cardiovascular diseases causing high morbidity and mortality represent a major socioeconomic burden. The primary cause of impaired heart function is often the loss of cardiomyocytes. Thus, novel therapies aim at restoring the lost myocardial tissue. One promising approach is cardiac tissue engineering. Previously, it is shown that *Antheraea mylitta* silk protein fibroin is a suitable material for cardiac tissue engineering, however, its quality is difficult to control. To overcome this limitation, the interaction of primary rat heart cells with engineered *Araneus diadematus* fibroin 4 ( $\kappa$ 16) (eADF4( $\kappa$ 16)) is investigated here, which is engineered based on the sequence of ADF4 by replacing the glutamic acid residue in the repetitive unit of its core domain with lysine. The data demonstrate that cardiomyocytes, fibroblasts, endothelial cells, and smooth muscle cells attach well to eADF4( $\kappa$ 16) films on glass coverslips which provide an engineered surface with a polycationic character. Moreover, eADF4( $\kappa$ 16) films have, in contrast to fibronectin films, no hypertrophic effect but allow the induction of cardiomyocyte hypertrophy. Finally, cardiomyocytes grown on eADF4( $\kappa$ 16) films respond to pro-proliferative factors and exhibit proper cell-to-cell communication and electric coupling. Collectively, these data demonstrate that designed recombinant eADF4( $\kappa$ 16)-based materials are promising materials for cardiac tissue engineering.


## 1. Introduction

The adult mammal is unable to regenerate heart tissue after an injury, resulting in the loss of cardiomyocytes, the contractile muscle cells of the heart.<sup>[1]</sup> Due to the major socioeconomic burden of cardiovascular disease, which has been predicted to further increase,<sup>[2]</sup> there is a great interest in the development of approaches to reverse the loss of cardiomyocytes. Promising approaches are the activation of endogenous stem cells, induction of cardiomyocyte proliferation, stem cell therapy, and cardiac tissue engineering.<sup>[3]</sup>

In recent years, cardiac tissue engineering has been established as a prospective option for the treatment of cardiac disease. In a landmark study, Zimmermann et al. showed that cardiomyocytes embedded in a nonstructured composite hydrogel made of type I collagen and Matrigel significantly improved heart function after implantation on myocardial infarcts in immune-suppressed rats.<sup>[4]</sup> Subsequently,

J. Petzold  
Department of Nephropathology  
Institute of Pathology  
Friedrich-Alexander-Universität Erlangen–Nürnberg (FAU)  
Schwabachanlage 12, 91054 Erlangen, Germany  
T. B. Aigner  
Lehrstuhl Biomaterialien  
Universität Bayreuth  
Universitätsstraße 30, Bayreuth D-95447, Germany  
F. Touska, Prof. K. Zimmermann  
Klinik für Anästhesiologie am Universitätsklinikum Erlangen  
Friedrich-Alexander-Universität Erlangen–Nürnberg (FAU)  
Krankenhausstrasse 12, 91054 Erlangen, Germany  
Prof. T. Scheibel  
Lehrstuhl Biomaterialien  
Bayreuther Zentrum für Kolloide und Grenzflächen (BZKG)  
Bayreuther Zentrum für Bio-Makromoleküle (bio-mac)  
Bayreuther Zentrum für Molekulare Biowissenschaften (BZMB)  
Bayreuther Materialzentrum (BayMAT)  
Bayerisches Polymerinstitut (BPI)  
Universität Bayreuth  
Universitätsstraße 30, Bayreuth D-95447, Germany

Prof. F. B. Engel  
Department of Nephropathology  
Institute of Pathology  
Muscle Research Center Erlangen (MURCE)  
Friedrich-Alexander-Universität Erlangen–Nürnberg (FAU)  
Schwabachanlage 12, 91054 Erlangen, Germany  
E-mail: felix.engel@uk-erlangen.de

 The ORCID identification number(s) for the author(s) of this article can be found under <https://doi.org/10.1002/adfm.201701427>.

DOI: 10.1002/adfm.201701427

it has been confirmed that tissue-engineered cardiac patches can improve recovery from myocardial injury in small and large animal models.<sup>[5]</sup> Moreover, first clinical trials applying tissue engineering to heart disease patients have been performed. In the most recent trial, Menasché et al. delivered human embryonic stem cell-derived cardiac progenitor cells in a fibrin patch into heart failure patients, demonstrating the overall feasibility and safety of cardiac tissue engineering to treat heart failure.<sup>[6]</sup> Nevertheless, the field is still in its infancy and it remains to be shown that the application of tissue engineering can indeed improve heart function in heart failure patients.

Currently, cardiac tissue engineering faces many problems, such as: (i) the choice of cell type or combination of cell types to generate a cardiac patch; (ii) providing hierarchically structured scaffolds to enable vascularization of cardiac patches to enlarge graft sizes; (iii) connecting the graft to the host vascularization; (iv) ensuring electrical coupling within the graft; (v) electromechanically integrating the graft to avoid arrhythmia; and (vi) the correct choice of biocompatible scaffold material with proper hierarchical structures and mechanical characteristics.<sup>[3b,7]</sup>

Previously, it has been demonstrated that silk materials are excellently suited for tissue engineering applications.<sup>[8]</sup> Silk proteins are natural products which have several advantages compared to other materials that are currently used in cardiac tissue engineering. They can be fabricated into diverse morphologies. Moreover, silk materials have unique mechanical strength, biocompatibility, and silks exhibit noncytotoxic properties as well as low level of inflammatory response.<sup>[8,9]</sup> In addition, we have demonstrated that the natural *Antheraea mylitta* silk fibroin is a suitable material for cardiac tissue engineering.<sup>[10]</sup> It enables efficient attachment of cardiomyocytes without affecting their response to extracellular stimuli, promotes sarcomere alignment, synchronous contraction, and electrical coupling.<sup>[10]</sup> However, naturally obtained silk fibroins have also significant limitations. For example, *Antheraea mylitta* cannot efficiently be bred in captivity, and thus its silk fibroin cannot be mass-produced and the latter's quality depends on a variety of variables that cannot be controlled (e.g., feedstock quality and uptake). The resulting batch-to-batch variation of this natural polymer and the lack of suitable quantitative and qualitative in vivo analyses are some of the issues currently restricting its medical application.<sup>[8b]</sup>

In order to overcome these limitations, we utilized here genetically engineered spider silk proteins, which make it possible to provide new biopolymers with a complexity and functionality not found in nature. The cell membranes of animal cells contain negatively charged proteoglycans, glycolipids, and glycoproteins. Therefore, mammalian cells attach preferentially to polycationic surfaces.<sup>[11]</sup> Consequently, the aim of this study was to determine if engineered recombinant spider silk protein engineered *Araneus diadematus* fibroin 4 ( $\kappa$ 16) (eADF4( $\kappa$ 16)) processed into films with a polycationic surface is a suitable adhesive for cardiac cells.

## 2. Results and Discussion

### 2.1. Surface Properties of Recombinant Spider Silk Protein eADF4( $\kappa$ 16) Films

eADF4(C16) is engineered based on the sequence of ADF4, a component of the major ampullate silk of the European garden

spider, also called the dragline or “lifeline.” Previously, we have shown that polyanionic eADF4(C16) films are not suitable substrates for cell adhesion.<sup>[12]</sup> As the extracellular side of most mammalian cells is negatively charged and thus cells preferentially attach to polycationic surfaces,<sup>[11]</sup> we engineered a so-called  $\kappa$ -module by replacing the naturally occurring glutamic acid residue in the repetitive units of the ADF4 core domain with lysine: GSSAAAAAASGPGGYGPKNQGPSGPGGYG-PGGP (Figure 1a).<sup>[13]</sup> The  $\kappa$ -module was adjusted to *Escherichia coli* (*E. coli*) codon-usage and then repeated 16 times to mimic the repetitive core of ADF4. The product is the engineered positively charged spider silk protein eADF4( $\kappa$ 16) (Figure 1a).

In order to determine the interaction of cardiac cells with eADF4( $\kappa$ 16), glass coverslips were dip coated with eADF4( $\kappa$ 16) out of formic acid (Figure 1b). Successful coating of glass coverslips was confirmed by Hoechst 33342 staining, resulting in apparent background illumination (Figure S1a, Supporting Information). Previously, eADF4(C16) film coatings showed already the formation of thermodynamically stable  $\beta$ -sheet rich structure during solvent evaporation.<sup>[14]</sup> To assess the secondary structure content of eADF4( $\kappa$ 16) coated glass coverslips, ATR-FTIR measurements were performed (Figure 1c). Fourier self-deconvolution (FSD) was performed analyzing the amide I band according to Hu et al.<sup>[15]</sup> As expected, the here investigated eADF4( $\kappa$ 16) films showed a high  $\beta$ -sheet content ( $34 \pm 1\%$ ;  $\alpha$ -helix:  $9 \pm 0.4\%$ ; turns:  $26 \pm 2\%$ ; random coils:  $15 \pm 1\%$ ; side chains:  $16 \pm 2\%$ ), explaining its insolubility in water even without methanol post-treatment (Figure 1c).

To determine if the high  $\beta$ -sheet content results in a hydrophobic film–air surface as previously described for cast eADF4(C16) films on glass,<sup>[14b]</sup> we characterized the surface hydrophilicity of all tested protein surfaces by using water contact angle measurements (Figure 1d). As control, in addition to eADF4(C16)-coated glass coverslips, we utilized noncoated as well as glass coverslips coated with fibronectin (dissolved in water or phosphate-buffered saline (PBS)) and gelatin that are often used as adhesive for cardiomyocytes.<sup>[10,16]</sup> Coating with eADF4( $\kappa$ 16) as well as gelatin reduced the contact angle of glass ( $38^\circ \pm 9^\circ$  and  $29^\circ \pm 7^\circ$ , respectively, vs  $56^\circ \pm 5^\circ$ , Figure 1d). The contact angle on fibronectin-coated surfaces was in comparison quite hydrophobic ( $H_2O$ :  $111^\circ \pm 2^\circ$ , PBS:  $80^\circ \pm 7^\circ$ , Figure 1d). These data demonstrate that eADF4( $\kappa$ 16) films are hydrophilic. Thus, in contrast to cast eADF4(C16) films on glass,<sup>[14b]</sup> eADF4( $\kappa$ 16) films are not covered by a layer of  $\beta$ -sheets (Figure 1b).

While we have previously shown that cast eADF4(C16) films on glass are hydrophobic,<sup>[14b]</sup> our data revealed that the eADF4(C16) film–air surface on silanized glass was more hydrophilic ( $54^\circ \pm 14^\circ$ , Figure 1d). Note that dip coating required the silanization of the glass coverslips, making them hydrophobic, in order to immobilize eADF4(C16) films. In contrast, eADF4( $\kappa$ 16) films directly adhered to glass surfaces upon dip coating.

Importantly, it is unknown at what water contact angles cardiomyocytes attach well. For fibroblasts, maximal cell adherence occurs at water contact angles between  $55^\circ$  and  $85^\circ$ .<sup>[17]</sup> However, it is known that the attachment of cells to surfaces is also strongly dependent on the presence of surface charges and functional groups.<sup>[11,18]</sup> Arginine-Glycine-Aspartic acid (Arg-Gly-Asp or RGD) domains, which are present in fibronectin, improve, for example, cardiomyocyte attachment.<sup>[10]</sup>

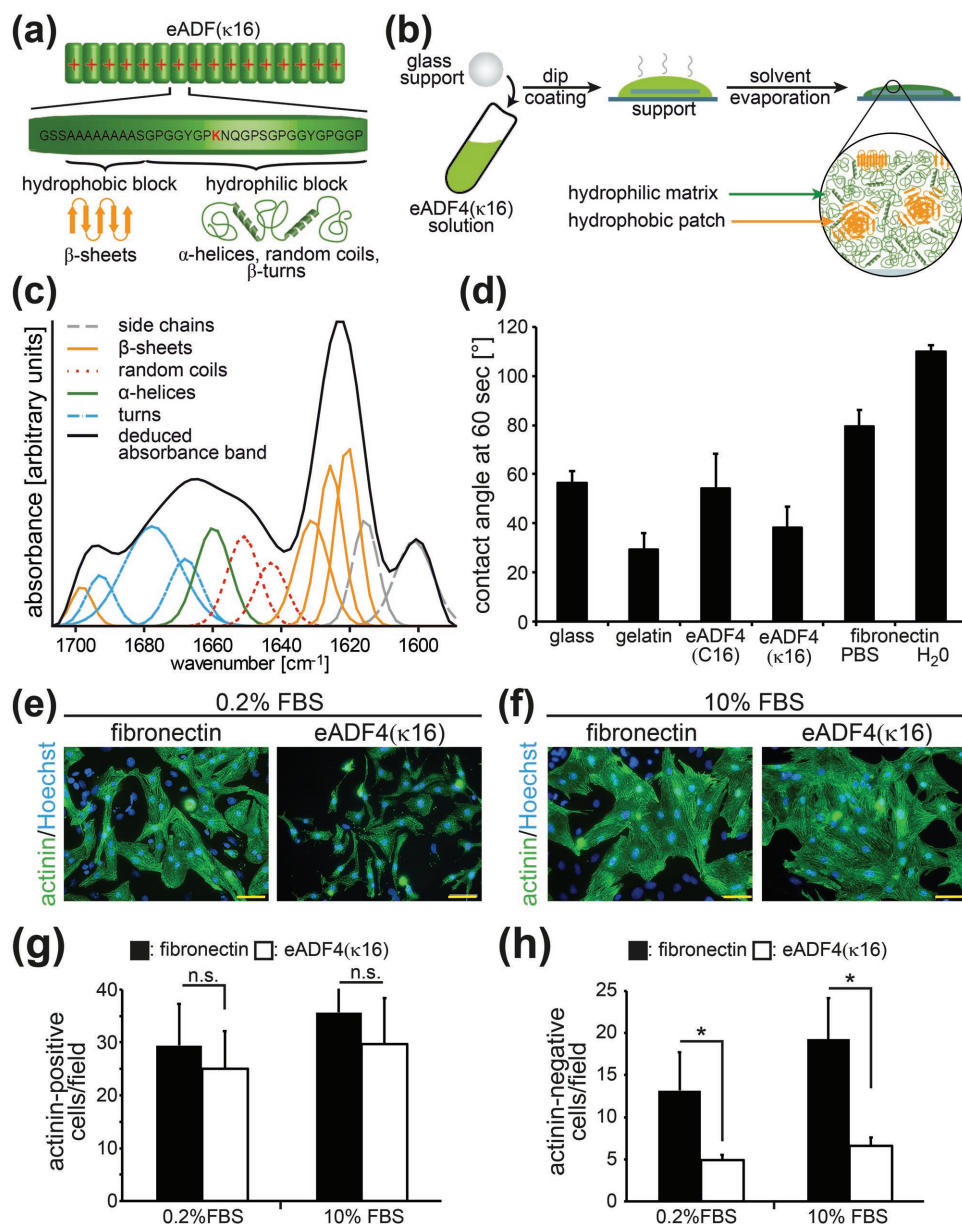


**Figure 1.** Cardiomyocytes efficiently attach to eADF4(κ16) films. a) Design of eADF4(κ16). b) Processing of eADF4(κ16) into films. c) Fourier self-deconvoluted absorbance spectrum of the amide I band of a eADF4(κ16) film on glass. Black line: deduced absorbance band, others: individual contributions to the amide I band assigned according to values published in literature ( $n = 5$ ). d) Water contact angle measurements ( $n = 8-10$ ). e, f) Cardiac cells isolated from ventricles of 3 d old rats were cultured after attachment overnight for 48 h on the indicated matrices in the presence of 0.2% (e) or 10% FBS (f). Subsequently, cardiomyocytes were stained with sarcomeric-α-actinin (actinin, green) and Hoechst 33342 (nuclei, blue). g) Quantitative analysis of sarcomeric-α-actinin-positive cardiomyocytes. h) Quantitative analysis of sarcomeric-α-actinin-negative nonmyocytes. Data are mean  $\pm$  SD.  $n = 4$  independent experiments. \*:  $p < 0.05$ . n.s.: statistically not significant. Scale bars: 50  $\mu$ m.

## 2.2. Cardiomyocytes, Nonmyocytes, and Human Umbilical Vein Endothelial Cells (HUVECs) Attach to eADF4(κ16) Films

To determine if polycationic eADF4(κ16) films are a suitable adhesive for cardiac cells, cells from postnatal day 3 (P3) rat hearts were isolated and cultured on eADF4(κ16) films after attachment overnight for 48 h. In parallel to attachment assays, we performed live/dead assays to verify that the recombinant spider silk protein eADF4(κ16) exhibits no cytotoxic effect on

cardiac cells. Previously, it had already been demonstrated that engineered recombinant spider silk proteins based on ADF4 are nontoxic.<sup>[19]</sup> As control, adhesive fibronectin was chosen since it is a component of the cardiac extracellular matrix and a well-established material for neonatal cardiomyocyte attachment.<sup>[10,20]</sup> Moreover, we have previously demonstrated that it exhibits similar properties as *Antheraea mylitta* silk fibroin.<sup>[10]</sup> The cells were cultured in presence of 0.2% as well as 10% (v/v) fetal bovine serum (FBS) as 10% FBS is commonly used to seed

cardiomyocytes for improved attachment.<sup>[21]</sup> However, 10% FBS is known to induce hypertrophy and/or cell cycle activity in neonatal cardiomyocytes as well as cardiomyocytes derived from human induced pluripotent stem cells.<sup>[22]</sup> Moreover, this hypertrophy might result in pathological hypertrophy.<sup>[23]</sup> Thus, it is pertinent to examine the effect of materials on cardiomyocytes also in culture media without or in low concentrations of serum.

Cells were stained with calcein-acetoxymethyl ester (calcein-AM) (0.25  $\mu\text{L mL}^{-1}$ )/ethidium homodimer-1 (EthD-1, 1  $\mu\text{L mL}^{-1}$ )/PBS (live/dead assay) (Figure S2, Supporting Information). Our data demonstrate that cardiac cells attach to eADF4( $\kappa$ 16) films (Figure S2a,b, Supporting Information). Moreover, there was no statistically significant difference in the number of attached calcein-AM-positive (live) or EthD-positive (dead) cells per field between eADF4( $\kappa$ 16) and fibronectin films ( $n = 3$  independent experiments,  $p > 0.2$ ; Figure S2c,d, Supporting Information). These data suggest that eADF4( $\kappa$ 16)-based materials are suitable for cardiac tissue engineering. In contrast, cardiomyocytes attached as expected poorly to polyanionic eADF4(C16) as previously shown for fibroblasts (Figure S2e,f, Supporting Information).<sup>[12]</sup>

It is important to note that the heart contains a large variety of cell types including fibroblasts, endothelial cells, smooth muscle cells, and cardiomyocytes.<sup>[24]</sup> Thus, we assessed next whether cardiomyocytes, the primary functional cell type of the heart, attach to eADF4( $\kappa$ 16) films. After cell isolation and cardiomyocyte enrichment, cells were allowed to attach overnight. After 48 h of culture in the presence of 0.2% or 10% FBS, cell cultures were stained for the cardiomyocyte-specific protein sarcomeric- $\alpha$ -actinin (Figure 1e,f). Quantitative analyses revealed that cardiomyocytes equally efficiently attached to eADF4( $\kappa$ 16) films as to fibronectin films (Figure 1g).

Previously, it has been shown that cardiac patches that contain both cardiomyocytes and nonmyocytes exhibit improved tissue structure and function.<sup>[25]</sup> In addition, vascularization of cardiac patches is required to ensure cardiomyocyte survival.<sup>[7a]</sup> Consequently, it is important to assess if also nonmyocytes can attach to eADF4( $\kappa$ 16)-based materials. A closer analysis of the cardiomyocyte attachment data revealed that the number of nonmyocytes (sarcomeric- $\alpha$ -actinin-negative) on eADF4( $\kappa$ 16) films was significantly lower than on fibronectin films (0.2% FBS:  $4 \pm 1$  vs  $10 \pm 5$  nonmyocytes; 10% FBS:  $7 \pm 1$  vs  $18 \pm 5$  nonmyocytes; data are mean  $\pm$  standard deviation (SD),  $n = 4$  independent experiments,  $p < 0.05$ ; Figure 1h). To determine if the most important cell types for cardiac tissue engineering (cardiomyocytes, endothelial cells, fibroblasts, and smooth muscle cells) can attach to eADF4( $\kappa$ 16) films, cardiac cells were isolated without cardiomyocyte enrichment. Cells were allowed to attach for 3 h as well as 48 h. Subsequently, cells were stained with cell type-specific markers to identify cardiomyocytes (sarcomeric- $\alpha$ -actinin or troponin I), fibroblasts (collagen 1), smooth muscle cells (smooth muscle actin), and endothelial cells (vascular endothelial- (VE)-cadherin). Our data demonstrate that fibroblasts (yellow arrowheads, Figure 2a), smooth muscle cells (blue arrowheads, Figure 2b), as well as endothelial cells (orange arrowheads, Figure 2c) can attach to eADF4( $\kappa$ 16) films. However, the data suggest that nonmyocytes attached less efficiently to eADF4( $\kappa$ 16) than to fibronectin films.

As the number of endothelial cells in the cultures was low, we tested whether eADF4( $\kappa$ 16) films are suitable for the attachment of HUVECs, which are often used to investigate the proangiogenic effect of materials or to engineer vessels.<sup>[26]</sup> HUVECs were cultured on eADF4( $\kappa$ 16) as well as fibronectin films and stained for VE-cadherin. HUVECs attached to and grew on both matrices to 100% confluency (Figure 2d). VE-cadherin staining on both matrices indicated a narrow adherens junction architecture. Collectively, our data demonstrate that eADF4( $\kappa$ 16) films allow not only the attachment of cardiomyocytes but also of other cell types present in the heart. The fact that nonmyocytes attach less to eADF4( $\kappa$ 16) films might be of advantage considering that they proliferate in contrast to cardiomyocytes. Thus, the use of eADF4( $\kappa$ 16) might be beneficial in generating cardiac tissue patches with a higher concentration of cardiomyocytes.

### 2.3. eADF4( $\kappa$ 16) Films Have No Hypertrophic Effect but Allow Cardiomyocytes to Respond to Hypertrophic Stimuli

Hearts, and especially cardiomyocytes, respond to a variety of extracellular stimuli that modulate heart function. For example, cardiomyocytes undergo physiological hypertrophy (increase in cell size) induced by hormones and growth factors that are released upon increased workload in athletes or during pregnancy.<sup>[23]</sup> To determine if eADF4( $\kappa$ 16) affects cardiomyocyte hypertrophy, we assessed cell size by determining the area of individual cardiomyocytes. While fibronectin is an obvious control for cardiomyocyte attachment, it is not the right negative control to determine whether a material exhibits a prohypertrophic effect as it has been demonstrated that fibronectin induces hypertrophy on neonatal cardiomyocytes and contributes to pathophysiological hypertrophy *in vivo*.<sup>[27]</sup> Therefore, we utilized gelatin, a commonly used and cheap moderate adhesive for cardiomyocytes,<sup>[10,16]</sup> as it has so far not been described to exhibit a prohypertrophic effect. In agreement with these data, we observed that the size of neonatal cardiomyocytes on fibronectin films was increased 1.34-fold compared to that of cardiomyocytes on gelatin films at low serum conditions (0.2% FBS,  $n = 3$  independent experiments,  $p < 0.05$ , Figure 3a,d). Cardiomyocytes cultured on eADF4( $\kappa$ 16) films were similar in size to cardiomyocytes cultured on films made of inert gelatin (1.05-fold,  $n = 3$  independent experiments,  $p > 0.05$ , Figure 3a,d). These data suggest that eADF4( $\kappa$ 16) films exhibit no pharmacological effect.

In order to assess whether neonatal cardiomyocytes on eADF4( $\kappa$ 16) films respond properly to hypertrophic stimuli, we subjected cardiomyocytes to a weak ( $50 \times 10^{-6}$  M phenylephrine, PE) as well as a strong hypertrophic stimulus (10% FBS) (Figure 3b,c). Quantitative analyses of cell size showed that neonatal cardiomyocytes on all matrices stimulated with 10% FBS increased significantly in cell size by around twofold ( $n = 3$  independent experiments,  $p < 0.05$ , Figure 3d). While stimulation with PE also showed a trend toward increased cell size, the change was not statistically significant. It should be noted that cell size was measured based on cross-sectional area which neglects that cells can also grow in size by increasing their thickness. Moreover, cross-sectional area is greatly affected



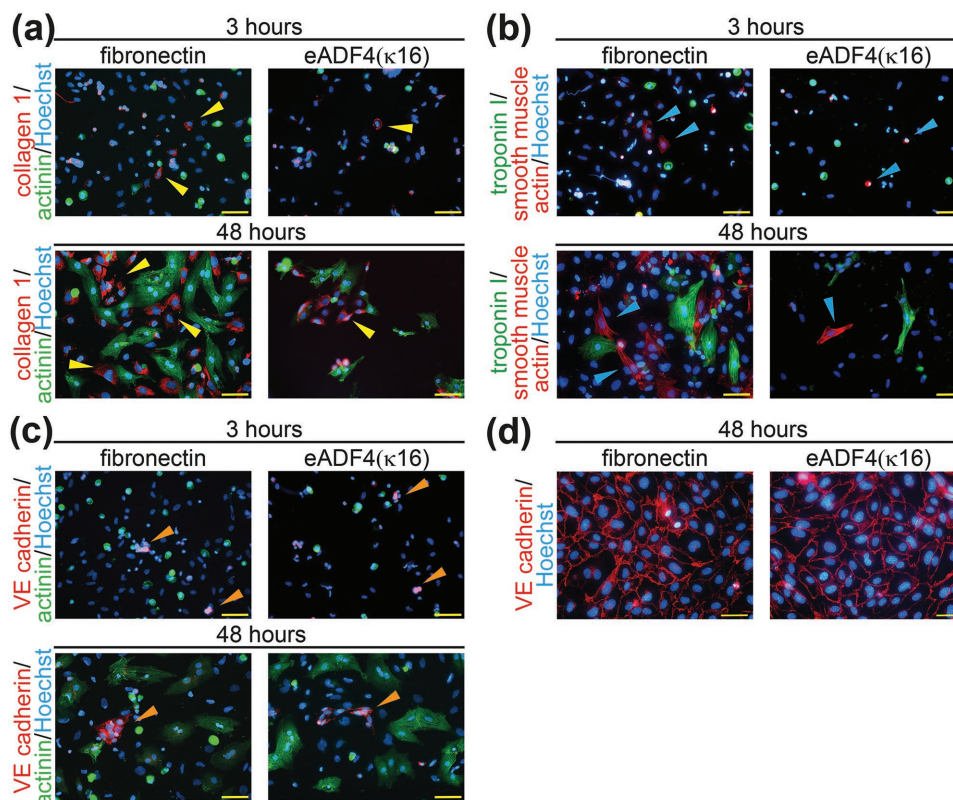


**Figure 2.** Nonmyocyte attachment on eADF4( $\kappa$ 16) films. Isolated neonatal rat cardiac cells (no enrichment) were seeded for 3 or 48 h on different matrices as indicated. a–c) Cells were stained with (a) anti-collagen 1 antibodies (fibroblasts, red) and anti-sarcomeric- $\alpha$ -actinin (cardiomyocytes, green), (b) anti-smooth muscle actin (marks smooth muscle cells and a subpopulation of cardiomyocytes, red) and anti-troponin I (cardiomyocytes, green), and (c) anti-VE-cadherin antibodies (endothelial cells, red) and anti-sarcomeric- $\alpha$ -actinin (cardiomyocytes, green). Nuclei were visualized with Hoechst 33342 (blue). Yellow arrowheads: examples of fibroblasts. Blue arrowheads: examples of smooth muscle cells. Orange arrowheads: examples of endothelial cells. d) HUVEC cell culture on matrices as indicated stained for VE-cadherin (red) and nuclei (Hoechst 33342, blue). Scale bars: 50  $\mu$ m.

by cell density. Therefore, we stained cardiomyocytes in parallel for atrial natriuretic factor (ANF, also atrial natriuretic peptide, ANP), which is expressed around the nucleus in hypertrophic cardiomyocytes.<sup>[28]</sup>

Quantitative analysis of ANF-positive cardiomyocytes indicates also that only fibronectin films exert a prohypertrophic effect ( $n = 3$  independent experiments,  $p < 0.05$ , Figure 3e). Moreover, ANF expression analyses revealed that cardiomyocytes on all matrices responded to 10% FBS as well as PE. Note that cardiomyocytes on gelatin and on eADF4( $\kappa$ 16) films responded in a similar manner to both stimulations in regards to cell size and ANF expression ( $n = 3$  independent experiments,  $p > 0.05$ , Figure 3d,e). Collectively, these data indicate that eADF4( $\kappa$ 16) is an inert material exhibiting no pharmacological effect but allows cardiomyocytes to respond properly to hypertrophic stimuli.

#### 2.4. Cardiomyocytes on eADF4( $\kappa$ 16) Films Respond Properly to Pro-Proliferative Stimuli

A current problem in cardiac tissue engineering is to generate cardiac tissues containing high densities of cardiomyocytes.<sup>[10,29]</sup> This is due to the problem of seeding 3D

scaffolds with cardiomyocytes or printing bioinks with high cell densities. Thus, it might be of advantage to utilize proliferative factors to promote cardiomyocyte proliferation in the generated constructs to increase cardiomyocyte density and thus contractility. Previously, it has been shown that stimulation of cardiomyocytes with FBS or fibroblast growth factor 1 (FGF1) plus an inhibitor of the mitogen-activated protein kinase p38 (p38i) induces cell cycle re-entry in neonatal as well as adult cardiomyocytes resulting in the synthesis of deoxyribonucleic acid (DNA).<sup>[30]</sup> Our data demonstrate that FBS, in a concentration-dependent manner, as well as FGF1/p38i, induce DNA synthesis in cardiomyocytes attached to eADF4( $\kappa$ 16) or fibronectin films (white asterisks, incorporation of the nucleoside analog of thymidine 5-ethynyl-2'-deoxyuridine (EdU), **Figure 4**), with no statistically significant difference between the two matrices (Figure 4d). These data indicate that eADF4( $\kappa$ 16) is a neutral substrate that does not influence cardiomyocyte behavior but permits the proper response of cardiomyocytes to extracellular stimuli. In addition, we observed that cardiomyocytes stimulated with FGF1/p38i exhibited on eADF4( $\kappa$ 16) an elongated morphology, a similar phenotype as previously observed for neonatal and adult cardiomyocytes cultured on the inert substrate gelatin (see also Figure S3a in the Supporting Information).<sup>[30a]</sup>

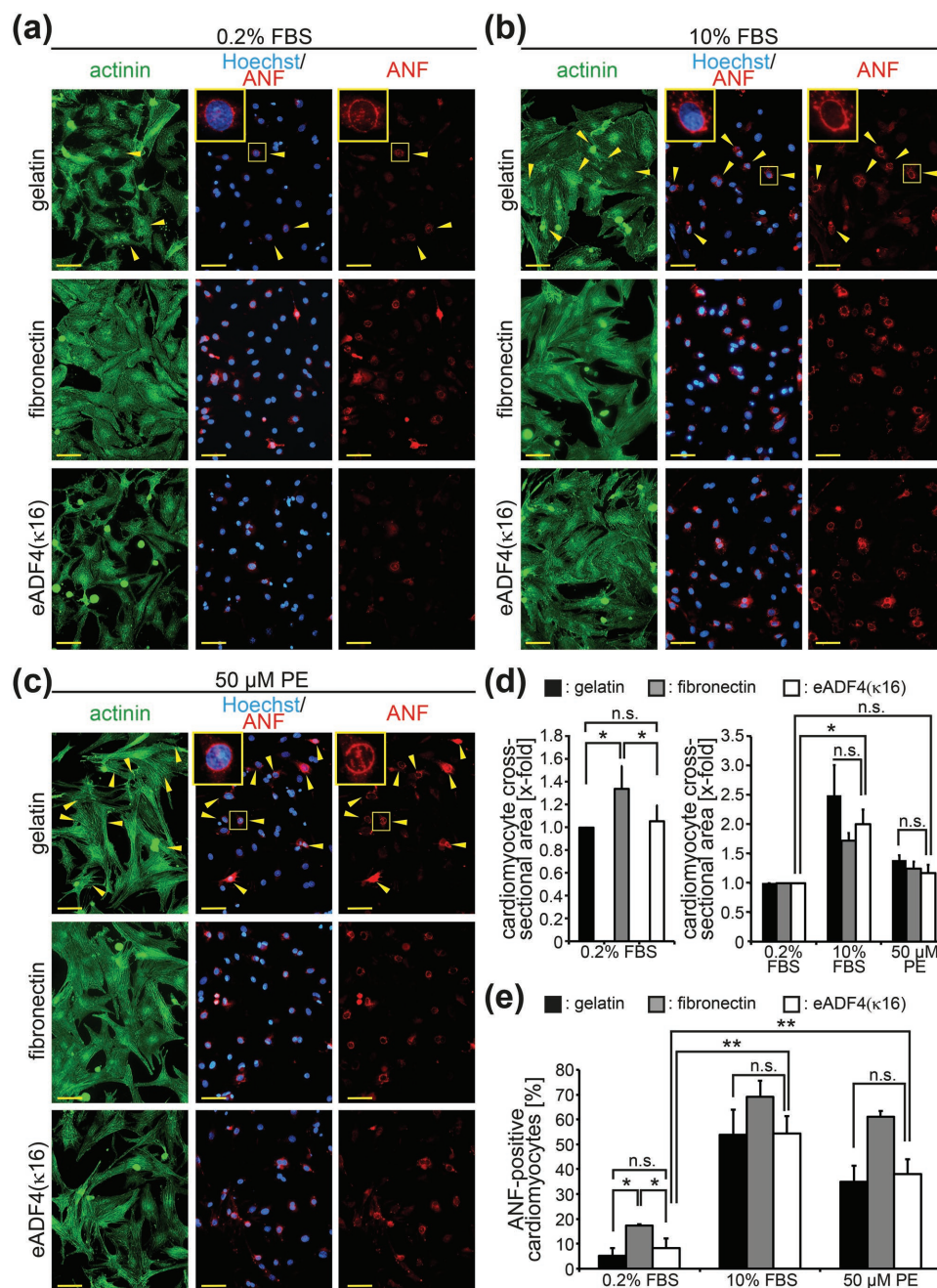


**Figure 3.** Cardiomyocytes respond properly to prohypertrophic stimuli on eADF4( $\kappa$ 16) films. Cardiomyocytes were stimulated with 0.2% or 10% FBS or  $50 \times 10^{-6}$  M phenylephrine (PE) and analyzed for a hypertrophic response (perinuclear ANF expression, cross-sectional area). a–c) Cardiomyocytes stained for sarcomeric- $\alpha$ -actinin (green), ANF (red), and DNA (Hoechst 33342, nuclei, blue). Yellow arrowheads: examples of ANF-positive cardiomyocytes exhibiting a clear perinuclear ANF signal (see inserts). d) Quantitative analysis of the cross-sectional area of sarcomeric- $\alpha$ -actinin-positive cardiomyocytes. Left panel: fold-change in relation to the mean cardiomyocyte size on gelatin films. Right panel: fold-change in relation to the mean cardiomyocyte size upon 0.2% stimulation on the respective matrix. e) Quantitative analysis of the number of ANF-/sarcomeric- $\alpha$ -actinin-positive cardiomyocytes ( $n = 3$  independent experiments, mean  $\pm$  SD, \*:  $p < 0.05$ , \*\*:  $p < 0.01$ . n.s.: statistically not significant). Scale bars: 50  $\mu$ m.

## 2.5. Cardiomyocytes on eADF4( $\kappa$ 16) Films Exhibit Proper Cell-to-cell Communication and Contractility

Since the major function of the heart is to contract, it is important to assess if cardiomyocytes contract well on eADF4( $\kappa$ 16) films. To allow high contractility, it is crucial that

cardiomyocytes exhibit well-differentiated sarcomeres. This was observed in all our experiments based on the staining of sarcomeric proteins (Figure S3b,c, Supporting Information). In addition, we utilized the fact that neonatal cardiomyocytes exhibit spontaneous contractile activity and recorded movies of cultures grown on eADF4( $\kappa$ 16) and fibronectin films and analyzed



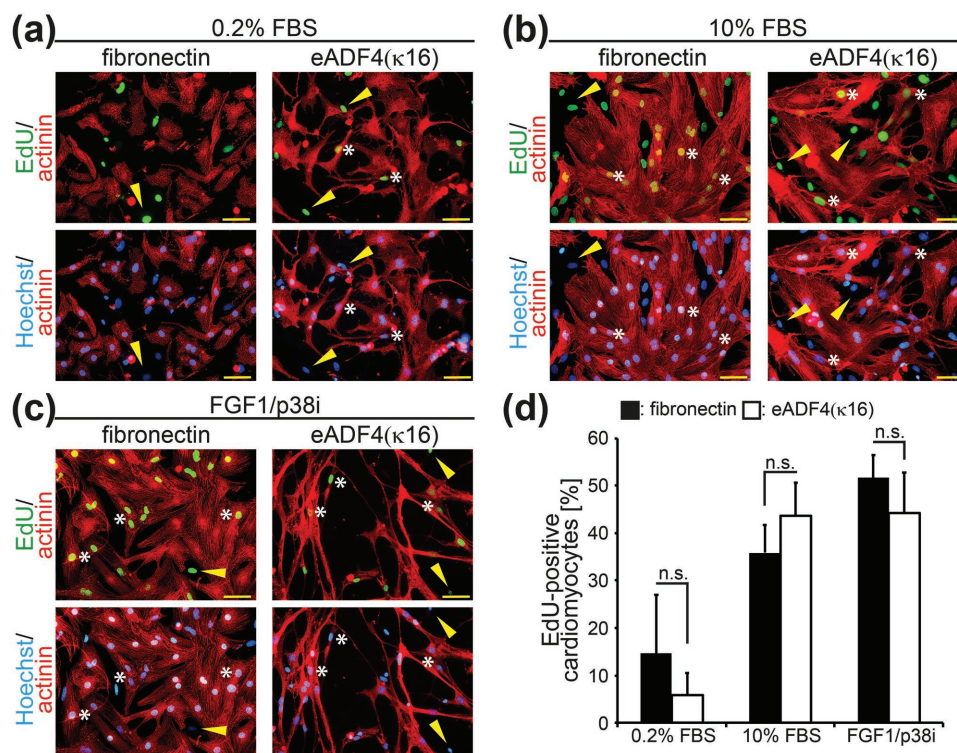


**Figure 4.** Cardiomyocytes respond properly to pro-proliferative stimuli on eADF4( $\kappa$ 16) films. Cardiomyocytes were stimulated with 0.2% or 10% FBS or FGF1 and a p38 inhibitor (p38i) and analyzed for DNA synthesis (EdU incorporation). a–c) Cardiomyocytes stained for sarcomeric- $\alpha$ -actinin (red), EdU (green), and DNA (Hoechst 33342, nuclei, blue). White asterisks: examples of EdU-positive cardiomyocytes. Yellow arrowheads: examples of EdU-positive nonmyocytes. d) Quantitative analysis of the number of EdU/sarcomeric- $\alpha$ -actinin-positive cardiomyocytes ( $n = 3$  independent experiments, mean  $\pm$  SD, n.s.: statistically not significant). Scale bars: 50  $\mu$ m.

them via Kymograph analysis software (Image J). This analysis showed that cardiomyocytes contract with the same frequency on eADF4( $\kappa$ 16) films as on fibronectin films and exhibit no arrhythmia (Figure 5a,b and Movies S1 and S2 (Supporting Information)).

In addition to proper contractility, it is important to determine if cardiomyocytes can communicate and electrically couple with each other, as efficient contraction of the heart is coordinated by propagating excitation waves. To assess if cardiomyocytes grown on eADF4( $\kappa$ 16) films are able to couple electrically, cardiomyocyte cultures were stained for the gap junctional protein connexin 43, which takes part in regulating electrical signal propagation between cardiomyocytes.<sup>[31]</sup> Immunofluorescence analyses revealed that cardiomyocytes grown on eADF4( $\kappa$ 16) and fibronectin films expressed connexin 43 along cellular junctions. This was enhanced upon stimulation with 10% FBS (Figure 5c,d).

Finally, to test effects on the calcium homeostasis, cultures on either matrix were loaded with the  $\text{Ca}^{2+}$ -sensitive indicator Fura-2 AM. This allowed the visualization of  $\text{Ca}^{2+}$  carried excitation waves (Figure 5e–j). The number of contractions on either fibronectin or eADF4( $\kappa$ 16) films was not significantly different. The contraction frequency for cardiomyocytes cultured on fibronectin films was on average  $12 \pm 4 \text{ min}^{-1}$  ( $n = 15$ ) and for eADF4( $\kappa$ 16) films  $12 \pm 4$  ( $n = 16$ ) (data are mean  $\pm$  SD, Figure 5e). Peak amplitude of intracellular calcium was  $0.54 \pm 0.10$  (arbitrary units) on fibronectin films

( $n = 15$ ) and  $0.53 \pm 0.06$  on eADF4( $\kappa$ 16) films ( $n = 16$ ) (data are mean  $\pm$  SD, Figure 5f).

To visualize the changes of intracellular calcium, sample recordings were extracted from cardiomyocytes plated on fibronectin (Figure 5g and Movie S3 (Supporting Information)) or eADF4( $\kappa$ 16) films (Figure 5h and Movie S4 (Supporting Information)). Examples of local calcium minima (left panel) and peak calcium concentration (right panel) for cardiomyocytes grown on fibronectin or eADF4( $\kappa$ 16) films are shown in Figure 5i,j, respectively. In conclusion, these data demonstrate that cardiomyocytes grown on eADF4( $\kappa$ 16) films exhibit proper cell-to-cell communication and electric coupling.

### 3. Conclusion

We have demonstrated that eADF4( $\kappa$ 16) films exhibit adhesion properties for the most important cell types in cardiac tissue engineering (cardiomyocytes, endothelial cells, fibroblasts, and smooth muscle cells) comparable to that of films made of fibronectin, a component of the native extracellular matrix of the heart and well-established coating material for neonatal cardiomyocytes. In addition, our data show that eADF4( $\kappa$ 16) films are noncytotoxic and have no pharmacological effect. Moreover, cardiomyocytes grown on eADF4( $\kappa$ 16) films respond properly to extracellular stimuli and exhibit proper

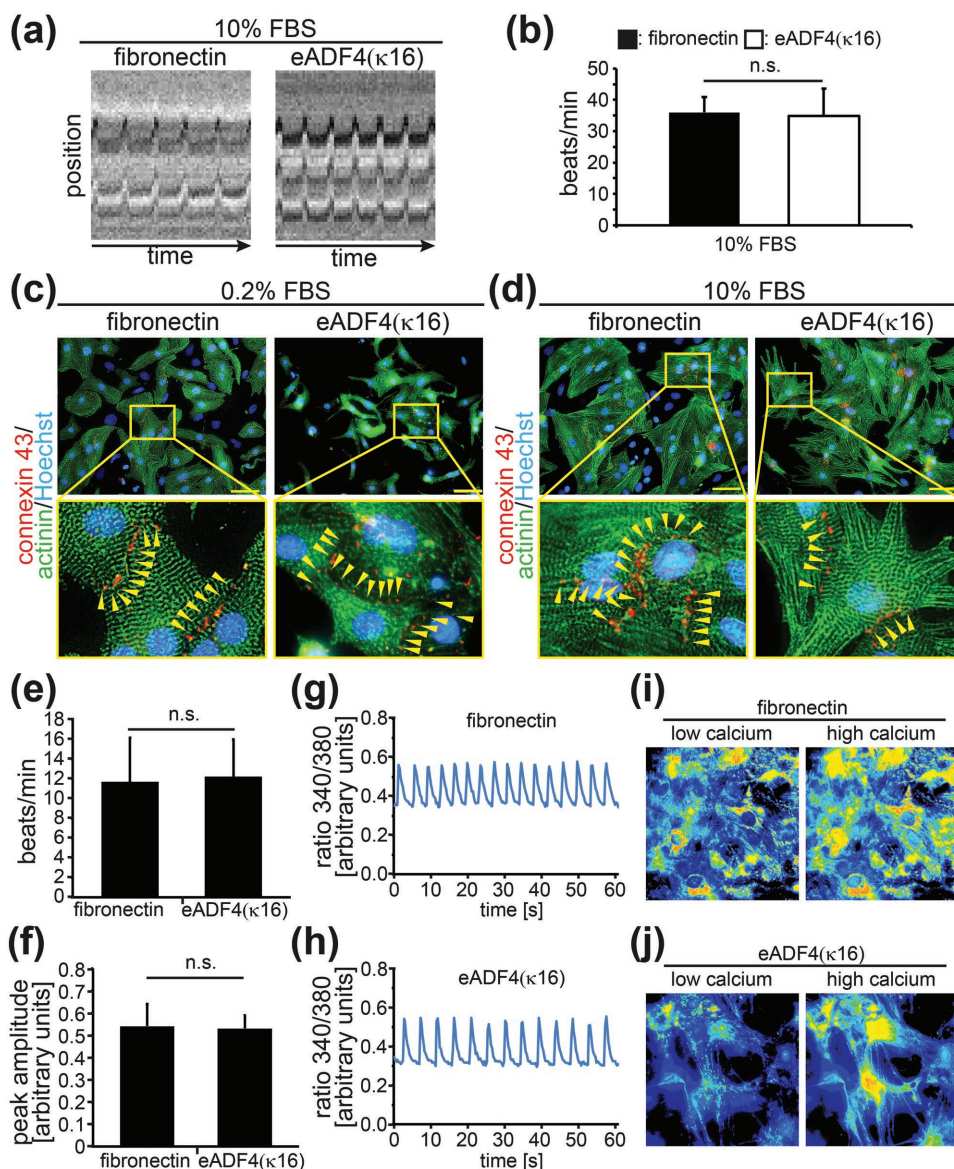


**Figure 5.** Cardiomyocytes on eADF4( $\kappa$ 16) films exhibit proper cell-to-cell communication and contractility. a) Example of Kymograph analysis visualizing contractions (peaks). b) Quantitative analysis of (a). c,d) Examples of cardiomyocytes seeded on different matrices stimulated with 0.2% (c) or 10% FBS (d) and subsequently stained for connexin 43 (red), sarcomeric- $\alpha$ -actinin (green) and DNA (Hoechst 33342, nuclei, blue). Note that cardiomyocytes on eADF4( $\kappa$ 16) films express connexin 43 (yellow arrowheads) suggesting well-established cell-to-cell communication. Ratiometric intracellular calcium imaging of cultured cardiomyocytes. e,f) Quantification of cardiomyocyte contraction frequency (e) and peak amplitude of intracellular calcium concentration (f) on fibronectin or eADF4( $\kappa$ 16) films. Note that the contraction frequency is lower than in (b) as data collection was performed at room temperature and in a different medium. g,h) Representative examples of intracellular calcium changes of cardiomyocytes cultured on either fibronectin (g) or eADF4( $\kappa$ 16) films (h). i,j) Representative images of local calcium minima (left panel) and peak calcium concentration (right panel) for cardiomyocytes cultured on either fibronectin (i) or eADF4( $\kappa$ 16) films (j). Left image depicts cardiomyocytes between contractions. Right image: depicts cardiomyocytes during contraction. Scale bars: 50  $\mu$ m.

excitation propagation. Our data demonstrate that eADF4( $\kappa$ 16) exhibits similar properties as fibronectin and thus also as *Antheraea mylitta* silk fibroin. In conclusion, we introduce the designed recombinant eADF4( $\kappa$ 16), previously developed for drug delivery applications,<sup>[13]</sup> as a new promising material for cardiac tissue engineering that also provides the known advantages of silk proteins<sup>[8,10]</sup> such as biodegradability<sup>[32]</sup> and low immunogenicity.<sup>[19c]</sup> As shown previously, eADF4 variants can be produced at large scale with high yields and high purity.<sup>[13]</sup>

Interestingly, eADF4( $\kappa$ 16) could in the future even be further genetically modified in order to optimize its performance as a substrate for cardiac tissue regeneration, for instance, by integrating additional functional domains.<sup>[12,33]</sup> Recombinant spider silk proteins can be processed into a diverse set of morphologies including fibers, foams, hydrogels, particles, nonwoven meshes, capsules, and films.<sup>[34]</sup> Moreover, we have recently demonstrated that cell-loaded recombinant spider silk bioinks can be printed by robotic dispensing without the



need for crosslinking additives or thickeners for mechanical stabilization,<sup>[35]</sup> it could be assessed whether it is possible to print stem-cell derived cardiomyocytes in eADF4( $\kappa$ 16)-based bioinks in order to biofabricate cardiac tissues for therapeutic applications.

## 4. Experimental Section

**Rat Neonatal Cardiomyocyte Isolation and Cell Culture:** The investigation conforms with the Guide for the Care and Use of Laboratory Animals published by the Directive 2010/63/EU of the European Parliament. Extraction of organs and preparation of primary cell cultures were approved by the local Animal Ethics Committee in accordance with governmental and international guidelines on animal experimentation (protocol TS—5/13 Nephropatho). Ventricular cardiac cells were isolated from 3 d old (P3) Sprague Dawley rats using the gentleMACS Dissociation kit (Milteny Biotec) according to the manufacturer's instructions. In order to isolate nonmyocytes, hearts were processed as previously reported.<sup>[36]</sup> For cardiomyocyte enrichment, cells were preplated for 90 min in Dulbecco's Modified Eagle Medium (DMEM)/F12 + GLUTAMAX (GIBCO) containing penicillin/streptomycin ( $100 \text{ U mg}^{-1} \text{ mL}^{-1}$ ) and FBS (10%). Nonattached cells, enriched in cardiomyocytes, were then collected, centrifuged for 5 min at  $330 \times g$ , resuspended in DMEM/F12 + GLUTAMAX containing penicillin/streptomycin ( $100 \text{ U mg}^{-1} \text{ mL}^{-1}$ ), and counted. Before seeding, serum was added as indicated in the figures or as described below. Cells were seeded in 24-well plates at a density of 150 000 cells after cardiomyocyte enrichment, 200 000 nonmyocytes, or 50 000 HUVECs per 500  $\mu\text{L}$  per well and were cultured at  $37^\circ\text{C}$  in a  $\text{CO}_2$ /air humidified atmosphere (5%/95%).

**Preparation of Silk:** The recombinant spider silk protein eADF4( $\kappa$ 16) consists of 16 repeats of a  $\kappa$ -module (sequence: GSSAAAAAASGPGGYGPKNQGPSPGGYGPGGP).<sup>[13]</sup> The spider silk protein was produced and purified as described before.<sup>[37]</sup> Briefly, eADF4( $\kappa$ 16) was produced in *E. coli* (BL21 gold), which was grown in a fed batch fermenter. The protein was purified using a heating step and ammonium sulfate precipitation.

**Coating Procedure:** Glass coverslips ( $\varnothing$  12 mm, Thermo Fisher Scientific) were placed in 24-well tissue culture plates, washed twice for 5 min with 70% ethanol, once with 100% ethanol for 5 min, and air dried under UV light for 30 min. For fibronectin-coating, coverslips were incubated with 100  $\mu\text{L}$  of fibronectin (Sigma-Aldrich, F1141)/PBS ( $25 \mu\text{g mL}^{-1}$ ) for 1 h at  $37^\circ\text{C}$ . Cells were seeded immediately after removing the remaining solution on the coverslips. For gelatin-coating, coverslips were incubated for 2 h at  $37^\circ\text{C}$  with 500  $\mu\text{L}$  gelatin (Sigma-Aldrich, G1890)/water (1%, w/v). Subsequently, the gelatin solution was replaced with fresh 500  $\mu\text{L}$  gelatin solution. After 2 h incubation at  $37^\circ\text{C}$ , the remaining solution on the coverslips was removed and coverslips were dried for another 1 h at  $37^\circ\text{C}$ . For spider silk-processing, purified and lyophilized eADF4( $\kappa$ 16) or eADF4(C16) was dissolved in formic acid and subsequently diluted with water (5:1, formic acid:water) to obtain a silk solution (0.34%, w/v). Coverslips were dip coated in this silk solution and dried on Parafilm M. Spider silk coatings from formic acid are water insoluble, therefore, further post-treatment was not necessary.<sup>[38]</sup> Before coating with eADF4(C16) (and only in that case), the coverslips were silanized with (3-aminopropyl) trimethoxysilane to prevent detachment of eADF4(C16) films due to electrostatic repulsion of the silk and plain glass. A homogeneous spreading of silk films was confirmed by subsequent Hoechst 33342-staining. For recording movies, cells were grown on eADF4( $\kappa$ 16)- or fibronectin-coated 8-well IBIDI slides. Note, eADF4( $\kappa$ 16)-coating was not performed as described above but according to another previously described method.<sup>[39]</sup> Briefly, purified and lyophilized eADF4( $\kappa$ 16) was dissolved in 1,1,1,3,3,3-hexafluoro-2-propanol (HFIP) and films were cast from a solution (2%, w/v) directly into the wells ( $0.15 \text{ mg cm}^{-2}$ ). After evaporation of HFIP, the water-soluble and  $\alpha$ -helix-rich films

were post-treated with ethanol in order to induce  $\beta$ -sheet formation, rendering them water-insoluble.<sup>[38]</sup>

**Water Contact Angle Measurements:** Coating was performed as described above with the following changes. All films were dried overnight on Parafilm. Fibronectin was diluted either in water (for better comparison to the other films) or PBS (as in the other experiments). Note that glass coverslips coated with fibronectin diluted in PBS were washed once with water before their transfer to Parafilm. Contact angles of coated glass coverslips were measured by sessile drop method at room temperature (RT) using a contact angle goniometer OCA-20 (DataPhysics Instruments, Filderstadt, Germany) and evaluated with the software SCA20-F. Uniform drops with a volume of 7  $\mu\text{L}$  were deposited using an automated dispensing system. The contact angles were determined 60 s after drop deposition using Young–Laplace algorithm. For each material, eight to ten measurements were performed ( $n = 8\text{--}10$ ).

**Attenuated Total Reflection-Fourier Transform Infrared (ATR-FTIR) Spectroscopy:** ATR-FTIR spectra of eADF4( $\kappa$ 16) films on glass and glass as control were measured in the range of  $4000\text{--}800 \text{ cm}^{-1}$  on a Ge-crystal with a Bruker Tensor 27 spectrometer (Bruker, Germany). For each spectrum, 100 scans were recorded at a resolution of  $4 \text{ cm}^{-1}$ . The secondary structure content was determined by analyzing the amide I region ( $1595\text{--}1705 \text{ cm}^{-1}$ ) with FSD using Opus software (Bruker, Germany) according to Hu et al.<sup>[15]</sup> Five samples were analyzed ( $n = 5$ ).

**Live/Dead Assay (Calcein-AM/Ethidium Homodimer-1):** Cells were seeded on coated coverslips, allowed to attach for 24 h, and after washing once with PBS, incubated in medium for another 48 h. Cells were then washed three times with PBS for 5 min and incubated with calcein-AM ( $0.25 \mu\text{L mL}^{-1}$ )/EthD-1 ( $1 \mu\text{L mL}^{-1}$ )/PBS (Life Technologies, L2334) for 10 min at  $37^\circ\text{C}$  in a  $\text{CO}_2$ /air humidified atmosphere (5%/95%). Subsequently, live images from ten randomly chosen microscopic fields ( $0.1 \text{ mm}^2$ ) per experiment were taken to quantify living and dead cells.

**Immunofluorescence Staining:** Cultured cells were fixed in formaldehyde (3.7%, Sigma-Aldrich; F1635) for 20 min. All antibodies were diluted in blocking buffer (5% Bovine Serum Albumin (BSA)/0.2% Tween 20/PBS) and all manipulations were carried out at RT. Samples were permeabilized for 10 min with Triton X-100/PBS (0.5%), blocked for 20 min in blocking buffer, and incubated for 1 h with primary antibodies. Primary antibodies used in this study were: mouse monoclonal anti-sarcomeric- $\alpha$ -actinin (Abcam, ab9465, 1:500), rabbit polyclonal anti-connexin 43 (Santa Cruz Biotechnology, sc-9059, 1:500), rabbit polyclonal anti-ANP/ANF (Phoenix Pharmaceuticals, H-005-24, 1:500), rabbit polyclonal anti-collagen 1 (Rockland, 600-401-103-0, 1:250), rabbit polyclonal anti-VE-cadherin (Abcam, ab33168, 1:200), rabbit polyclonal anti-Troponin I (Santa Cruz Biotechnology, sc-15368, 1:50), and mouse anti-smooth muscle actin (Sigma-Aldrich, A2547, 1:250). For EdU (a thymidine analog which will be incorporated into the DNA during DNA synthesis) incorporation assays, cells were seeded in 1% FBS and allowed to attach for 48 h. Cells were then washed with PBS and stimulated as indicated for 72 h. Note that the p38 inhibitor (p38i,  $10 \times 10^{-6} \text{ M}$ , SB203580-HCl, Tocris) was added every 24 h and that FGF1 ( $50 \text{ ng mL}^{-1}$ , R&D Systems)/p38i stimulation was in the presence of 0.2% FBS. EdU ( $30 \times 10^{-6} \text{ M}$ , Life Technologies, C10337) was added after 24 and 48 h. Cells were fixed after 72 h and stained for EdU according to manufacturer's instructions. Immune complexes were detected with ALEXA 488- or ALEXA 594-conjugated donkey anti-mouse or anti-rabbit antibodies (1:500, Life Technologies). DNA was visualized by incubation with Hoechst 33342 (1:5000/PBS) for 10 min.

**Cell Adhesion:** Cell adhesion was quantified by determining the average number of attached cells from ten randomly chosen microscopic fields ( $0.1 \text{ mm}^2$ ) per experiment.

**Hypertrophy Assay:** Cells were seeded in 0.2% FBS and allowed to attach for 24–48 h. Then, cells were washed and cultured in DMEM/F12 + GLUTAMAX containing  $100 \text{ U mg}^{-1} \text{ mL}^{-1}$  penicillin/streptomycin and 0.2% FBS, 10% FBS, or phenylephrine ( $50 \times 10^{-6} \text{ M}$ , Sigma-Aldrich, P6126). After 48 h, cells were fixed and ten randomly chosen microscopic fields ( $0.1 \text{ mm}^2$ ) per experiment were analyzed to determine the number of ANF-positive cardiomyocytes. In addition, the cross-sectional area of

at least 50 cardiomyocytes from five randomly chosen microscopic fields per experiment was determined via Photoshop.

**Movie Capture and Kymograph Analysis:** Movies of beating cardiomyocytes were recorded on a Keyence BZ9000 Fluorescence Microscope (Keyence, Osaka, Japan) and analyzed using the Image J Kymograph, which allows velocity measurements of moving structures in image time series. The x-axis of the kymograph is a time axis. A line in the kymograph in parallel to the x-axis indicates that there is no movement. A peak represents one contraction.

**Intracellular Calcium Imaging:** Cells were seeded in 10% FBS and allowed to attach for 48 h. Then, cells were washed once with PBS and cultured with DMEM/F12 + GLUTAMAX containing 100 U mg<sup>-1</sup> mL<sup>-1</sup> penicillin/streptomycin and 10% FBS for 5 d. Subsequently, cardiomyocyte medium was replaced with bathing solution (145 × 10<sup>-3</sup> M NaCl, 5 × 10<sup>-3</sup> M KCl, 1.25 × 10<sup>-3</sup> M CaCl<sub>2</sub>, 1 × 10<sup>-3</sup> M MgCl<sub>2</sub>, 10 × 10<sup>-3</sup> M 2-(4-(2-hydroxyethyl)-1-piperazinyl)-ethansulfonic acid (HEPES), 10 × 10<sup>-3</sup> M glucose, adjusted to pH 7.4 with NaOH) and loaded with Fura-2 AM (3 × 10<sup>-6</sup> M) (Invitrogen, USA) supplemented with 0.02% pluronic acid (Molecular Probes, USA). The cells were incubated for 30 min, followed by a 15 min washout period at 37 °C in a CO<sub>2</sub>/air humidified atmosphere (5%/95%). Afterward, cells were imaged within 5–15 min at RT. Several samples of three independent cultures were analyzed. Fura-2 AM was excited at 340 and 380 nm with 30 ms exposure time at 7 Hz sampling frequency using Lambda DG-4 Plus (Sutter Instrument, USA). Note that due to the measurement at RT and the different ionic composition of the incubation medium, the contraction frequency of cardiomyocytes was reduced. Ratiometric calcium imaging was performed using an Olympus IX83 microscope and acquired with a complementary metal-oxide-semiconductor (CMOS) camera (Orca-Flash4.0 LT, Hamamatsu, Japan) using SlideBook 6 software (3i, USA).

**Statistical Analysis:** Data are expressed as the mean ± SD of at least three independent experiments. Statistical significance of differences was evaluated by a two-tailed Student's *t*-test (Excel) or where appropriate by one way analysis of variance (ANOVA) followed by Bonferroni's post hoc test (GraphPad Prism). *p* < 0.05 was considered statistically significant.

## Supporting Information

Supporting Information is available from the Wiley Online Library or from the author.

## Acknowledgements

The authors would like to thank Robert Becker, Silvia Vargarajauregui, Kaveh Roshanbifar, Johannes Kramer, David Zebrowski, and Johannes Diehl for technical support and the lab of Michael Stürzl for providing HUVECs. This work was supported by the Deutsche Forschungsgemeinschaft (DFG, EN 453/11-1 and FOR2149 to F.B.E.), the Bavarian Research Foundation (DOK-175-15, to T.B.A.), and by the Bavarian Polymerinstitute Keylab Adaptive Biomanufacturing (to T.S.).

## Conflict of Interest

The authors declare no conflict of interest.

## Keywords

adhesion, cardiac tissue engineering, cell–material interactions, eADF4(κ16), engineered spider silk proteins

Received: March 17, 2017

Revised: June 2, 2017

Published online:

- [1] M. A. Laflamme, C. E. Murry, *Nature* **2011**, 473, 326.
- [2] D. Mozaffarian, E. J. Benjamin, A. S. Go, D. K. Arnett, M. J. Blaha, M. Cushman, S. R. Das, S. de Ferranti, J. P. Despres, H. J. Fullerton, V. J. Howard, M. D. Huffman, C. R. Isasi, M. C. Jimenez, S. E. Judd, B. M. Kissela, J. H. Lichtman, L. D. Lisabeth, S. Liu, R. H. Mackey, D. J. Magid, D. K. McGuire, E. R. Mohler 3rd, C. S. Moy, P. Muntner, M. E. Mussolino, K. Nasir, R. W. Neumar, G. Nichol, L. Palaniappan, D. K. Pandey, M. J. Reeves, C. J. Rodriguez, W. Rosamond, P. D. Sorlie, J. Stein, A. Towfighi, T. N. Turan, S. S. Virani, D. Woo, R. W. Yeh, M. B. Turner, *Circulation* **2016**, 133, e38.
- [3] a) R. Madonna, L. W. Van Laake, S. M. Davidson, F. B. Engel, D. J. Hausenloy, S. Lecour, J. Leor, C. Perrino, R. Schulz, K. Ytrehus, U. Landmesser, C. L. Mummery, S. Janssens, J. Willerson, T. Eschenhagen, P. Ferdinandy, J. P. Sluijter, *Eur. Heart J.* **2016**, 37, 1789; b) B. M. Ogle, N. Bursac, I. Dorian, N. F. Huang, P. Menasche, C. E. Murry, B. Pruitt, M. Radisic, J. C. Wu, S. M. Wu, J. Zhang, W. H. Zimmermann, G. Vunjak-Novakovic, *Sci. Transl. Med.* **2016**, 8, 342ps13; c) D. C. Zebrowski, R. Becker, F. B. Engel, *Am. J. Physiol.: Heart Circ. Physiol.* **2016**, 310, H1045; d) P. P. Zwetsloot, A. M. Vegh, S. J. Jansen of Lorkers, G. P. van Hout, G. L. Currie, E. S. Sena, H. Gremmels, J. W. Buikema, M. J. Goumans, M. R. Macleod, P. A. Doevendans, S. A. Chamuleau, J. P. Sluijter, *Circ. Res.* **2016**, 118, 1223.
- [4] W. H. Zimmermann, I. Melnychenko, G. Wasmeier, M. Didie, H. Naito, U. Nixdorff, A. Hess, L. Budinsky, K. Brune, B. Michaelis, S. Dhein, A. Schwoerer, H. Ehmke, T. Eschenhagen, *Nat. Med.* **2006**, 12, 452.
- [5] a) M. Kawamura, S. Miyagawa, K. Miki, A. Saito, S. Fukushima, T. Higuchi, T. Kawamura, T. Kuratani, T. Daimon, T. Shimizu, T. Okano, Y. Sawa, *Circulation* **2012**, 126, S29; b) Y. Shiba, S. Fernandes, W. Z. Zhu, D. Filice, V. Muskheli, J. Kim, N. J. Palpant, J. Gantz, K. W. Moyes, H. Reinecke, B. Van Biber, T. Dardas, J. L. Mignone, A. Izawa, R. Hanna, M. Viswanathan, J. D. Gold, M. I. Kotlikoff, N. Sarvazyan, M. W. Kay, C. E. Murry, M. A. Laflamme, *Nature* **2012**, 489, 322; c) F. Weinberger, K. Breckwoldt, S. Pecha, A. Kelly, B. Geertz, J. Starbatty, T. Yorgan, K. H. Cheng, K. Lessmann, T. Stolen, M. Scherrer-Crosbie, G. Smith, H. Reichenspurner, A. Hansen, T. Eschenhagen, *Sci. Transl. Med.* **2016**, 8, 363ra148.
- [6] P. Menasché, V. Vanneaux, A. Hagege, A. Bel, B. Cholley, I. Cacciapuoti, A. Parouchev, N. Benhamouda, G. Tachdjian, L. Tosca, J. H. Trouvin, J. R. Fabreguettes, V. Bellamy, R. Guillemain, C. Suberbielle Boissel, E. Tartour, M. Desnos, J. Larghero, *Eur. Heart J.* **2015**, 36, 2011.
- [7] a) C. Patra, A. R. Boccaccini, F. B. Engel, *Thromb. Haemostasis* **2015**, 113, 532; b) M. N. Hirt, A. Hansen, T. Eschenhagen, *Circ. Res.* **2014**, 114, 354.
- [8] a) D. Jao, X. Mou, X. Hu, *J. Funct. Biomater.* **2016**, 7, 22; b) B. Kundu, N. E. Kurland, S. Bano, C. Patra, F. B. Engel, V. K. Yadavalli, S. C. Kundu, *Prog. Polym. Sci.* **2014**, 39, 251.
- [9] A. E. Thurber, F. G. Omenetto, D. L. Kaplan, *Biomaterials* **2015**, 71, 145.
- [10] C. Patra, S. Talukdar, T. Novoyatleva, S. R. Velagala, C. Muhlfeld, B. Kundu, S. C. Kundu, F. B. Engel, *Biomaterials* **2012**, 33, 2673.
- [11] a) A. Blau, *Curr. Opin. Colloid Interface Sci.* **2013**, 18, 481; b) M. De Rosa, M. Carteni, O. Petillo, A. Calarco, S. Margarucci, F. Rosso, A. De Rosa, E. Farina, P. Grippo, G. Peluso, *J. Cell. Physiol.* **2004**, 198, 133.
- [12] S. Wohlrab, S. Muller, A. Schmidt, S. Neubauer, H. Kessler, A. Leal-Egana, T. Scheibel, *Biomaterials* **2012**, 33, 6650.
- [13] E. Doblhofer, T. Scheibel, *J. Pharm. Sci.* **2015**, 104, 988.

- [14] a) I. C. Um, H. Y. Kweon, K. G. Lee, Y. H. Park, *Int. J. Biol. Macromol.* **2003**, 33, 203; b) S. Wohlrab, K. Spiess, T. Scheibel, *J. Mater. Chem.* **2012**, 22, 22050.
- [15] X. Hu, D. Kaplan, P. Cebe, *Macromolecules* **2006**, 39, 6161.
- [16] C. Patra, F. Ricciardi, F. B. Engel, *Biomaterials* **2012**, 33, 4327.
- [17] Y. Tamada, Y. Ikada, *J. Biomed. Mater. Res.* **1994**, 28, 783.
- [18] M. J. Lydon, T. W. Minett, B. J. Tighe, *Biomaterials* **1985**, 6, 396.
- [19] a) C. B. Borkner, M. B. Elsner, T. Scheibel, *ACS Appl. Mater. Interfaces* **2014**, 6, 15611; b) A. Leal-Egana, T. Scheibel, *Biotechnol. Appl. Biochem.* **2010**, 55, 155; c) P. H. Zeplin, N. C. Maksimovikj, M. C. Jordan, J. Nickel, G. Lang, A. H. Leimer, L. Römer, T. Scheibel, *Adv. Funct. Mater.* **2014**, 24, 2658.
- [20] T. K. Borg, K. Rubin, E. Lundgren, K. Borg, B. Obrink, *Dev. Biol.* **1984**, 104, 86.
- [21] a) Y. Li, X. Shi, L. Tian, H. Sun, Y. Wu, X. Li, J. Li, Y. Wei, X. Han, J. Zhang, X. Jia, R. Bai, L. Jing, P. Ding, H. Liu, D. Han, *Adv. Mater.* **2016**, 28, 10230; b) S. R. Shin, B. Aghaei-Ghareh-Bolagh, X. Gao, M. Nikkhah, S. M. Jung, A. Dolatshahi-Pirouz, S. B. Kim, S. M. Kim, M. R. Dokmeci, X. S. Tang, A. Khademhosseini, *Adv. Funct. Mater.* **2014**, 24, 6136; c) S. R. Shin, R. Farzad, A. Tamayol, V. Manoharan, P. Mostafalu, Y. S. Zhang, M. Akbari, S. M. Jung, D. Kim, M. Comotto, N. Annabi, F. E. Al-Hazmi, M. R. Dokmeci, A. Khademhosseini, *Adv. Mater.* **2016**, 28, 3280; d) S. R. Shin, C. Shin, A. Memic, S. Shadmehr, M. Miscuglio, H. Y. Jung, S. M. Jung, H. Bae, A. Khademhosseini, X. S. Tang, M. R. Dokmeci, *Adv. Funct. Mater.* **2015**, 25, 4486.
- [22] a) C. Dambrot, S. R. Braam, L. G. Tertoolen, M. Birket, D. E. Atsma, C. L. Mummery, *J. Cell. Mol. Med.* **2014**, 18, 1509; b) M. Qi, K. Ojamaa, E. G. Eleftheriades, I. Klein, A. M. Samarel, *Am. J. Physiol.* **1994**, 267, C520; c) J. Sadoshima, H. Aoki, S. Izumo, *Circ. Res.* **1997**, 80, 228.
- [23] I. Shimizu, T. Minamino, *J. Mol. Cell. Cardiol.* **2016**, 97, 245.
- [24] a) I. Banerjee, J. W. Fuseler, R. L. Price, T. K. Borg, T. A. Baudino, *Am. J. Physiol.: Heart Circ. Physiol.* **2007**, 293, H1883; b) H. W. Vliegen, A. van der Laarse, C. J. Cornelisse, F. Eulderink, *Eur. Heart J.* **1991**, 12, 488.
- [25] H. Naito, I. Melnychenko, M. Didie, K. Schneiderbanger, P. Schubert, S. Rosenkranz, T. Eschenhagen, W. H. Zimmermann, *Circulation* **2006**, 114, 172.
- [26] a) S. Zhao, L. Li, H. Wang, Y. Zhang, X. Cheng, N. Zhou, M. N. Rahaman, Z. Liu, W. Huang, C. Zhang, *Biomaterials* **2015**, 53, 379; b) Z. Zhao, J. Wang, J. Lu, Y. Yu, F. Fu, H. Wang, Y. Liu, Y. Zhao, Z. Gu, *Nanoscale* **2016**, 8, 13574.
- [27] M. H. Konstandin, M. Volkers, B. Collins, P. Quijada, M. Quintana, A. De La Torre, L. Ormachea, S. Din, N. Gude, H. Toko, M. A. Sussman, *Basic Res. Cardiol.* **2013**, 108, 375.
- [28] C. Putinski, M. Abdul-Ghani, R. Stiles, S. Brunette, S. A. Dick, P. Fernando, L. A. Megeney, *Proc. Natl. Acad. Sci. USA* **2013**, 110, E4079.
- [29] a) R. Gaetani, P. A. Doevendans, C. H. Metz, J. Alblas, E. Messina, A. Giacomello, J. P. Sluijter, *Biomaterials* **2012**, 33, 1782; b) R. Gaetani, D. A. Feyen, V. Verhage, R. Slaats, E. Messina, K. L. Christman, A. Giacomello, P. A. Doevendans, J. P. Sluijter, *Biomaterials* **2015**, 61, 339; c) J. Jang, H. J. Park, S. W. Kim, H. Kim, J. Y. Park, S. J. Na, H. J. Kim, M. N. Park, S. H. Choi, S. H. Park, S. W. Kim, S. M. Kwon, P. J. Kim, D. W. Cho, *Biomaterials* **2017**, 112, 264.
- [30] a) F. B. Engel, M. Schebesta, M. T. Duong, G. Lu, S. Ren, J. B. Madwed, H. Jiang, Y. Wang, M. T. Keating, *Genes Dev.* **2005**, 19, 1175; b) F. B. Engel, M. Schebesta, M. T. Keating, *J. Mol. Cell. Cardiol.* **2006**, 41, 601.
- [31] P. A. Guerrero, R. B. Schuessler, L. M. Davis, E. C. Beyer, C. M. Johnson, K. A. Yamada, J. E. Saffitz, *J. Clin. Invest.* **1997**, 99, 1991.
- [32] a) A. Lammel, M. Schwab, M. Hofer, G. Winter, T. Scheibel, *Biomaterials* **2011**, 32, 2233; b) S. Müller-Herrmann, T. Scheibel, *ACS Biomater. Sci. Eng.* **2015**, 1, 247.
- [33] K. Schacht, T. Scheibel, *Curr. Opin. Biotechnol.* **2014**, 29, 62.
- [34] a) J. G. Hardy, T. R. Scheibel, *Biochem. Soc. Trans.* **2009**, 37, 677; b) E. Doblhofer, A. Heidebrecht, T. Scheibel, *Appl. Microbiol. Biotechnol.* **2015**, 99, 9361.
- [35] K. Schacht, T. Jungst, M. Schweinlin, A. Ewald, J. Groll, T. Scheibel, *Angew. Chem. Int. Ed.* **2015**, 54, 2816.
- [36] F. B. Engel, L. Hauck, M. C. Cardoso, H. Leonhardt, R. Dietz, R. von Harsdorf, *Circ. Res.* **1999**, 85, 294.
- [37] D. Huemmerich, C. W. Helsen, S. Quedzuweit, J. Oschmann, R. Rudolph, T. Scheibel, *Biochemistry* **2004**, 43, 13604.
- [38] K. Spiess, R. Ene, C. D. Keenan, J. Senker, F. Kremer, T. Scheibel, *J. Mater. Chem.* **2011**, 21, 13594.
- [39] A. Leal-Egana, G. Lang, C. Mauerer, J. Wickinghoff, M. Weber, S. Geimer, T. Scheibel, *Adv. Eng. Mater.* **2012**, 14, 867.